MOLECULAR ECOLOGY

Molecular Ecology (2016) doi: 10.1111/mec.13842

SPECIAL ISSUE: MICROBIAL LOCAL ADAPTATION

Modified niche optima and breadths explain the historical contingency of bacterial community responses to eutrophication in coastal sediments

S. FODELIANAKIS,*† A. MOUSTAKAS,‡ N. PAPAGEORGIOU,† O. MANOLI,† I. TSIKOPOULOU,† G. MICHOUD,* D. DAFFONCHIO,* I. KARAKASSIS† and E. D. LADOUKAKIS†

Biological and Environmental Sciences and Engineering Department, King Abdullah University of Science and Technology (KAUST), Thuwal 23955-6900, Saudi Arabia, †Department of Biology, University of Crete, Voutes University Campus, 70013 Heraklion, Crete, Greece, ‡School of Biological and Chemical Sciences, Queen Mary University of London, Mile End Road, London E1 4NS, UK

Abstract

Previous studies have shown that the response of bacterial communities to disturbances depends on their environmental history. Historically fluctuating habitats host communities that respond better to disturbance than communities of historically stable habitats. However, the exact ecological mechanism that drives this dependency remains unknown. Here, we experimentally demonstrate that modifications of niche optima and niche breadths of the community members are driving this dependency of bacterial responses to past environmental conditions. First, we develop a novel, simple method to calculate the niche optima and breadths of bacterial taxa regarding single environmental gradients. Then, we test this method on sediment bacterial communities of three habitats, one historically stable and less loaded and two historically more variable and more loaded habitats in terms of historical chlorophyll-α water concentration, that we subject to hypoxia via organic matter addition *ex situ*. We find that communities containing bacterial taxa differently adapted to hypoxia show different structural and functional responses, depending on the sediment's environmental history. Specifically, in the historically less fluctuating and loaded sediments where we find more taxa poorly adapted to hypoxic conditions, communities change a lot over time and organic matter is not degraded efficiently. The opposite is true for the historically more fluctuating and loaded sediments where we find more taxa well adapted to hypoxia. Based on the community responses observed here, we also propose an alternative calculation of community resistance that takes into account how rapidly the communities respond to disturbances and not just the initial and final states of the community.

Keywords: adaptation, bacterial communities, community resistance, disturbance, environmental history

Received 10 April 2016; revision received 30 August 2016; accepted 14 September 2016

Introduction

With a total biomass similar to that of all the plants on earth combined, bacteria play a central role in the cycling of carbon and nutrients in the biosphere (Whitman *et al.* 1998). Examining how bacterial communities respond to environmental stress is integral to determine their contributions to the different ecosystem services in the global scale (Peralta *et al.* 2014b). Therefore, there is high scientific value in understanding what drives the structural and functional responses of bacterial communities.

Currently, empirical evidence suggests that past environmental fluctuations can constrain the responses of bacterial communities to environmental disturbance in soils and sediments (Bouskill *et al.* 2013; Peralta *et al.*

Correspondence: Stilianos Fodelianakis, Fax: +966 2 808 2377; E-mail: stelios.fodelianakis@kaust.edu.sa

2013, 2014a), but the underlying ecological mechanism is still unknown. Environmental history could modify the abiotic parameters of a soil or sediment system such as, among others, the grain size, the water holding capacity or the porosity of a soil matrix, for example, by the deposition of organic matter or inorganic minerals through time (Barbier *et al.* 2010). Thus, community responses could be constrained just because of the differences in the environmental parameters among systems with different environmental histories. Alternatively, environmental history could alter the preferences (niche optima) and the degree of specialization (niche breadths) of the bacterial taxa within a community, and that could also constrain community responses because communities from historically stable environments would be 'less trained' to disturbances. Recent results from an *in silico* modelling study support the latter, showing that when communities that contain taxa with random niche parameters are exposed to varying levels of historical environmental heterogeneity, functional constraints manifest (Hawkes & Keitt 2015). This process would result in communities with distinct niche parameters, as per their environmental history. However, this has not been examined experimentally for real bacterial communities yet.

Such a task is challenging because it requires the determination of the niche parameters of each taxon within bacterial communities, which are usually very diverse (Sogin *et al.* 2006). This can be done by examining the response of community members along environmental gradients, but in field studies many environmental variables become spatially autocorrelated, and therefore, the effect of a single gradient can be hard to measure (Langenheder & Ragnarsson 2007; Langenheder *et al.* 2011; Caporaso *et al.* 2012; Lindström & Langenheder 2012). Therefore, experiments that involve the quantification of the effects of single environmental gradients on bacterial communities can benefit from the more controlled environment of laboratory experiments (Vellend 2010; Hanson *et al.* 2012; Lindström & Langenheder 2012; Nemergut *et al.* 2013; Srivastava & Kratina 2013).

Here, we designed and performed a laboratory experiment to empirically examine how past environmental conditions drive the bacterial community's structural and functional response to disturbances. We focused on bacterial communities of coastal sediments that we exposed to hypoxia, which was mediated by the addition of organic matter. Coastal sediments are buffer zones where organic matter and nutrient flow is regulated between terrestrial and marine environments (Barbier *et al.* 2010). As a consequence of human-related activities, coastal ecosystems are frequently subjected to organic enrichment. This often leads to eutrophication that is characterized by the increased chlorophyll-α (chl-α) concentration and oxygen depletion in the water column and in the top sediment (millimetres to centimetres, depending on the habitat) that is, otherwise, oxic (Diaz & Rosenberg 2008). Thus, organic matter loading, eutrophication of the water column and hypoxia at the top sediment are interconnected at coastal habitats.

We hypothesized that sediment communities from historically more fluctuating environments in terms of eutrophication (in this study: the estuary and marina habitats, Fig. 1A) would be structurally and functionally more resistant to hypoxia (Fig. 1B) compared with communities from historically less fluctuating habitats (in this study: the beach habitat, Fig. 1A). With that in mind, we also sought to revise the way that community resistance is calculated so that the rate of the response is taken into account, along with the initial and final community states. Moreover, we hypothesized that the historically more fluctuating habitats would possibly contain more hypoxia-acclimated (in the ecological sense) bacterial taxa (Fig. 1C), because the latter could have likely encountered hypoxic conditions more often. Environmental history could be especially important in controlling the responses of coastal sedimentary habitats, because sediment bacteria experience temporal variability in a more static manner compared with water column bacteria, the latter being subjected to much greater environmental variability due to the current transport than due to seasonality (Doblin & van Sebille 2016). Moreover, because sediments are considerably isolated spatially (Zinger *et al.* 2014), environmental rescue by arrival of new community members is less frequent and the role of local interactions in shaping the resident bacterial communities is strengthened (Büchi & Vuilleumier 2014).

We added organic matter *ex situ* (Table 1) to induce hypoxia in bacterial communities from three coastal habitats originating from the same parent material (shale; Dornsiepen & Manutsoglu 1994; Zachariasse *et al.* 2008) but experiencing different chl-α historical fluctuations in the water column (Fig. 1A) and having different sediment characteristics (Table 2) and distinct communities (see Results). The eastern Mediterranean Sea is an ultra-oligotrophic basin (Krom *et al.* 2005). Therefore, although none of the examined sites can be considered historically eutrophic in a global scale, the historical differences in chl-α levels among the examined sites represent extremities on a local scale. We developed a novel, simple computational method by which we calculated the niche optima and breadths of the bacterial taxa in each community concerning a single parameter, in our case the sediment redox potential (Eh). Then, we assessed the communities' structural and functional responses to organic enrichment through time. We observed that not only community functional and structural responses were constrained by the

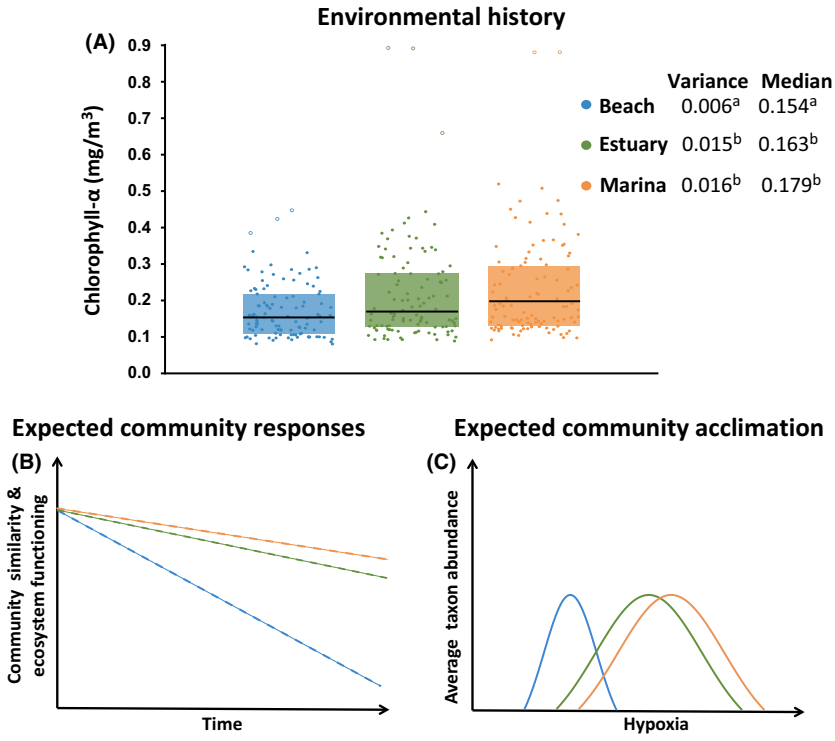

Fig. 1 Historical chlorophyll-α data and expected results according to our hypothesis. (A) Chlorophyll-α levels in the water column at the three sites for 106 months prior to sampling (n = 106). The horizontal line represents the median, the coloured boxes represent the 25th–75th percentile, and the open circles are the outlier values. a and b superscript letters indicate different levels of median and variance values. (B) The expected structural and functional responses of each community to eutrophication. (C) The expected community-wise niche optima and niche breadths of the communities.

Table 1 The four incubation conditions in this study; treatments 1 and 2 are control treatments, and treatments 3 and 4 are eutrophication treatments

	Water column aeration	
	No	Yes
Organic enrichment		
No	Treatment 1	Treatment 2
Yes	Treatment 3	Treatment 4

Table 2 The initial characteristics of the sediments at each site

	Silt & clay (%)	MD (mm)	TOM (% w/w)	Eh
Beach	0	0.3	1.78 ± 0.09	409
Estuary	19.46	0.16	7.61 ± 0.48	74
Marina	0.77	0.22	3.57 ± 0.17	239

Standard error is given after the ± symbol where applicable (n = 3).
MD, median grain size; TOM, total organic matter; Eh, the redox potential at the water–sediment interface.

environmental history, but also that the latter led to communities with different niche optima and breadths.

Materials and methods

Study sites and sampling strategy

Coastal sediment was collected in May 2011 from three sites along the North coast of the Greek Island, Crete: a beach (35°24′9.58″N, 24°57′12.82″E), an estuary (35°20′21.59″N, 25°6′44.74″E) and a marina (35°21′12.35″N, 25°2′34.10″E; see Fig. S8, Supporting information for details). Replicate cores at each site were collected following a 3 m × 4 m systematic unaligned grid sampling (grid cell dimensions were 1 m × 1 m; Wollenhaupt & Wolkowski 1994). Historical water column chl-α levels were significantly different between the beach and the estuary and between the beach and the marina, but not between the estuary and the marina (Fig. 1A, Supporting information).

At a water depth of ~1 m, we sampled the upper 15 cm of the sediment with sterilized cylindrical PVC corers (9.4 cm internal diameter). Twelve core samples were collected from each site, sealed with rubber stoppers and transferred to the laboratory in a vertical position within 1 h after sampling. Sediment samples were also collected *in situ* (t_{-1}) for DNA extraction, granulometry analysis and determination of organic matter content. Sediment temperature and Eh at the water–sediment interface were also measured *in situ*.

Ex situ organic enrichment experimental set-up

In the laboratory, each core was placed in one of 12 microcosms (50-L capacity) in a controlled temperature

chamber. Three replicate cores from the same sampling site were placed vertically in each microcosm, each of which was filled with 35 L of sterile saline water (35 g/L NaCl) before removing the rubber stoppers. The water level within each chamber was at least 10 cm above the rim of the cores at all times throughout the experiment. The chamber was illuminated with cold white light (6500 K) with a photoperiod of 12 h and temperature was fixed to incubate the cores at the *in situ* temperature on the day of sampling (19 °C).

Cores were left to settle for 24 h and then (t_0) incubated for 32 days under four different treatments: two control treatments and two treatments provided with supplementary organic matter to represent different eutrophication scenarios. Samples in treatment 1 (Tr1) received no organic enrichment or water column aeration; those in treatment 2 (Tr2) received no organic enrichment, but did receive water column aeration; those in treatment 3 (Tr3) received organic enrichment in the absence of water column aeration; and those in treatment 4 (Tr4) received both organic enrichment and water column aeration (Table 1).

Three microcosms (one per site), each containing three cores from the same sampling site, were incubated under the conditions of each treatment (Fig. S9, Supporting information). We acknowledge that this experimental manipulation resulted in pseudoreplication of each [site × treatment] combination because the different cores within the same mesocosm cannot be considered entirely independent; they are subject to the effects of the same mesocosm.

Organic enrichment was achieved by adding 0.31 g of sterilized fish food pellets once every 2 days (starting on t_0) at the top sediment as described elsewhere (Valdemarsen *et al.* 2009). Aeration of the water column was performed with air pumps at a high input rate (~10 L/min). Salinity was measured and fixed on a daily basis with the addition of sterile distilled water. For each core, changes in bacterial community structure (through 16S rRNA gene Illumina amplicon sequencing), hydrogen sulphide, organic matter content, Eh and dissolved oxygen at the water column were monitored on t_0 and every 4 days throughout the experiment (i.e. eight samplings within 32 days). Sampling was always performed before organic matter addition on experimental days 0, 4, 8, 12, 16, 20, 24, 28 and 32. Sampling was performed on the top half centimetre of the sediment from each core, with all possible effort to minimize the external contamination.

Environmental parameter monitoring

Historical water column chl-α concentration data from the three sites were obtained from the NASA AQUA-MODIS website (http://oceancolor.gsfc.nasa.gov/cgi/l3) and chl-α values were calculated with the use of the OCI algorithm (Hu *et al.* 2012) in the System for AUTOMATED GEOSCIENTIFIC ANALYSES software version 2.2. The data for all sites fit a normal distribution (Table S1 and Fig. S9, Supporting information), but did not have homogenous variances, and therefore, Mann–Whitney pairwise tests were used to identify the differences in the median values between sites. Methodological details are given in Supporting Information.

We measured Eh with an electrode standardized with Zobell's solution (ZoBell 1946) and sulphide concentration at the water–sediment interface using an electrode (Orion Sure-Flow™ Combination Ag^+/S^{2-} Electrode), as described elsewhere (Wildish *et al.* 1999). Labile organic matter (LOM) and refractory organic matter (ROM) contents of each sample and of the homogenized fish food were distinguished by the 'loss on ignition' method (Loh *et al.* 2008). Total organic matter (TOM – used for *in situ* samples) content was defined as TOM = LOM + ROM. Sediment granulometry analysis to determine the median grain size (MD) and the sand and silt/clay fractions was performed through dry sieving. Temperature was measured with a standard mercury thermometer.

Bacterial community structure monitoring

DNA was extracted from the sediment using a combination of mechanical lysis and chemical lysis followed by isolation and purification (Roose-Amsaleg *et al.* 2001). Polymerase chain reaction of the V4 hypervariable region of the 16S rRNA gene using primers 515f (5′-GTGCCAGCMGCCGCGGTAA-3′) and 806r (5′-GGACTACHVGGGTWTCTAAT-3′; Caporaso *et al.* 2011) and Illumina sequencing were performed at the U.S. Department of Energy Joint Genome Institute (DOE JGI) following the standard protocols for the Human Microbiome Project (http://hmpdacc.org/micro_analysis/microbiome_analyses.php) for bidirectional sequencing on a MiSeq platform. Noise filtering and sequence clustering into operational taxonomic units (OTUs) were also performed at the DOE JGI using the UClust algorithm (Edgar 2010). OTUs with 97% sequence similarity are commonly used as an equivalent for bacterial species (Mariadassou *et al.* 2015). In total, 263 samples of the total possible 333 samples were included in the final analysis. The rest 70 samples were excluded due to core losses during sampling, unsuccessful PCR amplification or inadequate community coverage. For more information on DNA extraction, sequencing and noise filtering of the sequences, please see the Supporting Information.

Statistical analyses

To measure community coverage, we calculated a Good's coverage index for each sample in QIIME (Caporaso *et al.* 2010) version 1.8; any sample with an index below 0.9 was removed because such values indicate the inadequate community coverage (Good 1953). The Bray–Curtis (BC) similarity was calculated using the OTU table obtained from QIIME and the *vegdist* function of the vegan package (Oksanen *et al.* 2013) in R (R Development Core Team, 2014). Only OTUs that were taxonomically assigned to Bacteria were used for the BC calculation because Archaea are considerably underrepresented using primers 515f–806r (Klindworth *et al.* 2013). Prior to calculating the BC index, read counts, which conventionally represent the abundance of each taxon within each sample, were $\log(x + 1)$-transformed (where x is the read count). To compare the environmental parameters across treatments, sites and trough times, Spearman rank correlations, parametric and nonparametric *t*-tests were performed in the PAST 3.04 software version for Mac OS (Hammer *et al.* 2001), and *P*-values were Bonferroni-corrected when applicable. The analysis of similarity (ANOSIM) tests, which were used to test for significant grouping among *in situ* samples or among differently treated samples (i.e. enriched–nonenriched, aerated–nonaerated samples) during the experiment, were performed in PRIMER 6 (Clarke & Warwick 2001).

Community similarity decay. To assess the community similarity decay over time at each site, we calculated the BC similarity at each time point between each control organically enriched sample pair (i.e. all sample pairs between treatment 1 and treatment 3, treatment 1–treatment 4, treatment 2–treatment 3 and treatment 2–treatment 4). First, we used a generalized linear model to test whether the BC decay rate was different among the three sites (for details, please refer to Table S5, Supporting information). Then, we plotted the BC values against the corresponding experimental time points separately for each site to reveal whether the linear, quadratic, exponential or logistic model best fit the decay over time; the models were selected based on the Akaike information criterion (AIC) in R (Table S3, Supporting information). Graphical representation of the modelled BC decay and the 95% confidence intervals through time were performed in the PAST 3.04 software (Hammer *et al.* 2001). Community resistance (RS) for each site was also calculated as $RS = 1 - 2|BC_{t0} - BC_{t8}|/(BC_{t0} + |BC_{t0} - BC_{t8}|)$ (eqn 1; Shade *et al.* 2012), where BC_{t0} and BC_{t8} are the average BC values between each control organically enriched sample pair at the beginning and at the end of the experiment, respectively (n = 20–144 depending on the site and experimental time).

Ecosystem functioning. We assessed the organic matter dynamics over time as a means of ecosystem functioning at each site. To do this, we examined the ROM/LOM ratio over time for cores that received organic matter (treatments 3 and 4). We calculated the initial ROM/LOM ratio at each site (R_0) and the expected ROM/LOM ratio if no degradation of LOM occurred (R_e) (Supporting Information). The latter calculation was based on the consistency in organic matter of the fish food pellets that we added. Then, we examined the ROM/LOM values that we observed over the course of the experiment for the cores that received organic matter. In a well-functioning sedimentary bacterial community, LOM is degraded more rapidly than ROM because it is more bioavailable. Thus, in a well-functioning community, the ROM/LOM ratio should be greater than R_e. Alternatively, ROM/LOM ratio values close to R_e indicate that the bacterial community cannot effectively catabolize the available organic matter. To compare the ROM/LOM values against R_e, we used Wilcoxon tests, because the ROM/LOM values were not normally distributed. We compared the median of the ROM/LOM values at each site across all experimental days against the R_e.

To correct for sampling errors imposed by the nature of the experiment, we chose to use the ROM/LOM ratio rather than the LOM percentage alone. For example, bias in the total organic matter content of a sample could arise from accidental 'scooping' of remaining fish food aggregates during sampling, despite thoroughly homogenizing the fish food. Although this potential error could create LOM estimation biases, it would not create a bias in the ROM/LOM ratio. We also plotted the ROM/LOM ratio at the different incubation times for nonorganically enriched samples (samples from treatments 1 and 2) of each different site, as an additional control. We assumed that the degradation of organic matter was mostly performed by bacteria, because we observed a rapid switch to anaerobic conditions (Figs S1–S6, Supporting information) where the activity of eukaryotic organisms such as macrofauna is limited (Furukawa *et al.* 2004).

Community acclimation to hypoxia. To examine whether the bacterial communities at the different sites contained bacteria with different environmental preferences (with respect to hypoxia), we developed a simple model by which we calculated the niche optimum and breadth of each bacterial taxon. Although here we applied the model along a redox potential (Eh) gradient at the water–sediment interface, the method is not specific for Eh and thus it can be used to calculate the niche parameters of bacterial taxa along other environmental gradients. The bacterial taxa correspond to operational

taxonomic units (OTUs), which are defined as groups of sequences with 97% similarity, or more, using 16S rRNA gene amplicon sequencing. OTUs with 97% sequence similarity are commonly used as an equivalent for bacterial species (Mariadassou *et al.* 2015). For each OTU, the model uses the OTU's relative abundance profile along the environmental gradient (in our case Eh, Fig. 2) to calculate the following three parameters.

xmax. The value of the environmental gradient at the sample where the examined OTU's relative abundance is the highest among all samples. This value is used to indicate the preferred environment, that is the niche optimum, of each OTU. Based on this value, OTUs can be categorized into ecologically meaningful fractions. For example, here it was used to determine whether an OTU is *aerophilic* or *anaerophilic:* if xmax > 0, the OTU was categorized as aerophilic (e.g. Fig. 2 – OTU 1), and if xmax ≤ 0, the OTU was categorized as anaerophilic (e.g. Fig. 2 – OTU 0). It has to be noted that this approach does not exclude the contribution of other correlated abiotic or biotic factors (e.g. grazing or interactions among bacterial taxa) to shaping niche optima.

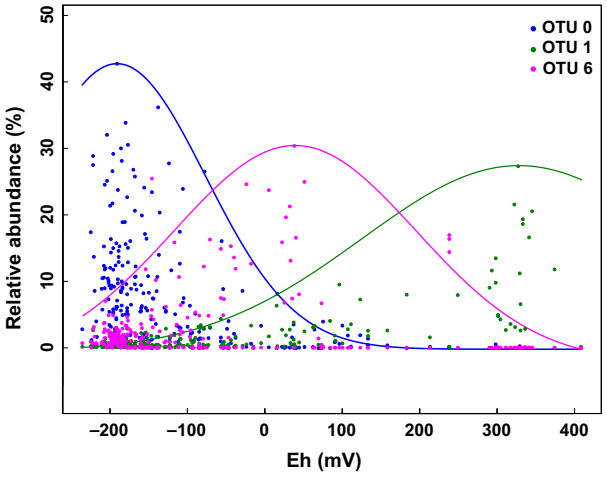

Fig. 2 Example of three modelled OTU distributions along the redox potential gradient at the water–sediment interface. OTU 0 is taxonomically affiliated to the family of *Pelobacteraceae*, OTU 1 is taxonomically affiliated to the bacterial family of *Vibrionaceae*, and OTU 6 is taxonomically affiliated to the bacterial family of *Campylobacteraceae*. Dots represent the observed relative abundance values (n = 263), and lines represent the modelled distributions, represented as normal distributions to enhance the visualization. The mean of each distribution was set to equal the niche optimum, that is the average Eh of the sample where the maximum relative abundance of the OTU was observed (xmax). The standard deviation was set to equal the niche breadth of each OTU, as defined in this study (dσ). The height (on the y-axis) of each distribution was set to equal the maximum relative abundance of each OTU (ymax).

ymax. The maximum relative abundance (% of total) of an OTU among all samples. High ymax values combined with small dσ values are indicative of specialist taxa, that is taxa that thrive in a narrow range of environmental conditions (Hawkes & Keitt 2015; e.g. OTU 0 in Fig. 2).

dσ. This parameter represents how rapidly the relative abundance of an OTU changes with respect to the environmental gradient. In other words, it describes how tolerant an OTU is to changes in the examined environmental parameter, that is, its niche breadth. If the distributions of the OTUs along the Eh gradient were normal, standard deviation would be an ideal indicator for this purpose; however, because the distributions of OTUs are largely heterogeneous, we needed a broader estimate of niche breadth. Therefore, we defined dσ as a broad analogue of the standard deviation (although qualitatively similar results were obtained independently of the choice of scaling factor): 34% of the maximum absolute difference between xmax $- x_1$ and xmax $- x_2$, where $x1$ and $x2$ are two environmental values of two samples, with $x_1 \leq$ xmax $\leq x_2$ and with the relative abundance of an OTU at $x1$ and $x2$, y_{x1} and y_{x2}, respectively, being equal to or greater than 5% of the ymax. We excluded any observation with relative abundance <5% of the ymax as it could artificially enlarge dσ. Mathematically expressed, dσ = 0.68*max|x1 − x2|/2, for those xs where $y_x \geq$ ymax/20 and $x_1 \leq$ xmax $\leq x_2$. The more generalist an OTU is concerning a single environmental gradient, the higher the $d\sigma$.

We determined whether the niche parameters for Eh, namely xmax, ymax and dσ, were phylogenetically conserved among OTUs to ensure that they are ecologically important (see the Supporting Information) by means of the K-statistic (Blomberg *et al.* 2003) implemented in the *picante* package (Kembel *et al.* 2010) in R. We plotted the xmax, ymax and dσ for the aerophilic and anaerophilic community fractions at each site as normal distribution plots with mean = xmax, sd = dσ and f(xmax) = ymax to improve visualization and to facilitate the comparison among sites. And finally, we plotted the relative abundance of three example OTUs along the Eh gradient (Fig. 2).

Results

The hypoxic gradient during the experiment was a major driver of bacterial dynamics

Results from *in situ* sampling showed different sediment characteristics and distinct bacterial communities at each site. The sediment at the estuary contained the highest percentage of silt and clay, the smallest median

grain size, the highest total organic matter content and the lowest redox potential (Table 2). The sediment at the beach was entirely coarse sand, which contained the lowest organic matter content and the highest redox potential, while the sediment at the marina showed intermediate values for these parameters (Table 2). The initial average Bray–Curtis similarity indices between sites were 25.08% (marina–estuary), 15.2% (marina–beach) and 10.9% (beach–estuary), with significant differences between communities at each site (ANOSIM test, $n = 8$, global $R = 0.612$, $P = 0.004$). The initial average within-site BC similarity indices were 54.43%, 46.12% and 44.29% for beach, marina and estuary samples, respectively.

The experimental manipulation resulted in a decrease in Eh during incubation followed by an increase in hydrogen sulphide emissions for all treatments and sediments (Figs S1–S6, Supporting information). The Eh at the water–sediment interface ranged between −235 and 375 mV during the experiment. Initially, Eh values were positive in all microcosms (337–375, 45–70 and 39–52 mV for beach, estuary and marina samples, respectively), but by the end of the experiment, Eh values were negative in all microcosms (−221 to −223, −220 to −235 and −224 to −235 mV for beach, estuary and marina samples, respectively). Organic matter addition had a strong and significant effect on community similarity (Bray–Curtis (BC) similarity) across all sites and experimental times (ANOSIM, global $R = 0.224$, $P < 0.001$). On the opposite, aeration had no significant effect on community similarity for any site or at any time (ANOSIM, global $R = 0.001$, $P = 0.391$). Collectively, these results suggest that oxygen availability in the sediments was limited by diffusion as reported elsewhere (Valdemarsen *et al*. 2009), irrespective of the treatment. However, the dissolved oxygen in the water column was lower in the microcosms that received organic matter compared with those that did not (Fig. S7, Supporting information), as typically occurs in the cases of eutrophication in nature (Diaz & Rosenberg 2008).

We used Eh as a descriptor of the eutrophication gradient because among all measured environmental variables (Eh, hydrogen sulphide emission; LOM, labile organic matter; and ROM, refractory organic matter), it explains most of the variance in bacterial communities at each site (12.8%–23%, $P < 0.01$, Table S6, Supporting information). Moreover, the niche optima (xmax) and breadths (dσ) of the OTUs along the Eh gradient exerted a strong phylogenetic signal ($K = 0.126$, $P = 0.001$; and $K = 0.142$, $P = 0.001$; for xmax and dσ, respectively). This indicates that niche parameters are phylogenetically conserved at the OTU level, meaning that phylogenetically more related OTUs have more similar niche parameters. However, the maximum relative abundance of an OTU (ymax) was not phylogenetically conserved ($K = 0.470$, $P = 1$).

The structural and functional community responses to eutrophication are linked to differently acclimated communities

The environmental preferences of OTUs regarding Eh were site dependent. Samples from the beach contained a total of 118 458 bacterial OTUs: 74 533 were anaerophilic; that is, their niche optimum was at hypoxic (Eh < 0) sediments, and 43 925 were aerophilic; that is, their niche optimum was at oxic (Eh > 0) sediments (~1.70 ratio). Samples from the other two sites contained a larger proportion of anaerophilic OTUs. Samples from the estuary contained a total of 110 572 bacterial OTUs: 92 893 were anaerophilic and 17 679 were aerophilic (~5.25 ratio). Samples from the marina contained a total of 100 275 bacterial OTUs: 75 001 were anaerophilic and 25 274 were aerophilic (~2.97 ratio). The niche parameters of the aerophilic and anaerophilic OTUs were also different among the different sites (Welch F tests, $P < 0.0001$ for all comparisons, Table S4, Supporting information), with the most profound differences being found among the aerophilic taxa of the different habitats (Fig. 3, dashed lines; Table 3). For example, communities from the beach contained aerophilic bacteria with little tolerance for decreased Eh and with a strong preference for oxic environments (Fig. 3, dashed blue line). On the contrary, the estuary and marina communities contained aerophilic bacteria with higher tolerance for decreased Eh and with less strong preference for oxic environments (Fig. 3, dashed green and orange lines).

The differences in the niche parameters of the bacterial OTUs among the sites were also concomitant with different structural and functional community responses depending on the sediment site of origin. The community similarity decreased exponentially among enriched/control samples at the beach (exponential decrease, $a = 26.94$, $b = -0.372$, $c = 23.15$, adjusted $R^2 = 0.573$, $n = 327$, $P = 2.1E{-}16$; Fig. 4A, left side), the site that historically had the lowest chl-α levels and variability in the water column among the three sites. The community resistance for the beach samples was measured at 0.233. In addition, the ROM/LOM ratio in the organically enriched samples from the beach did not differ significantly from the expected ratio if no LOM degradation occurred (Wilcoxon test, normal appr. $z = 0.681$, $P = 0.495$; Fig. 4B, left side). This indicates that the bacterial community could not effectively catabolize the added organic matter. The opposite was observed for the other two, historically more loaded and fluctuating, habitats. These communities changed

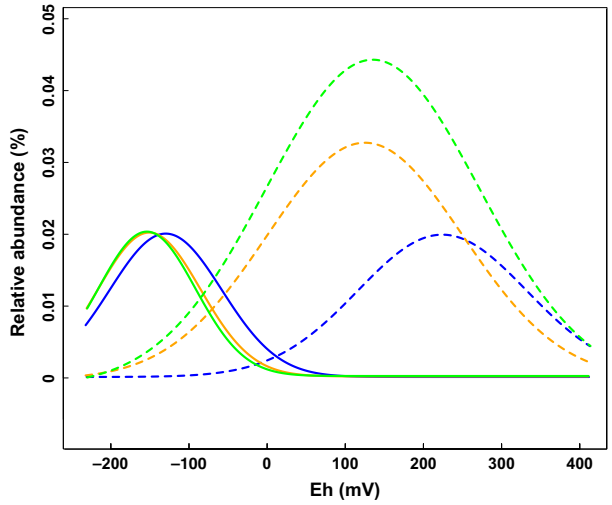

Fig. 3 The acclimation of the communities along the redox potential gradient at the water–sediment interface. Normal distribution plots of the niche parameters, xmax, ymax and dσ for aerophilic (dashed lines, n = 74 533, 17 679 and 25 274 for beach, estuary and marina samples, respectively) and anaerophilic (solid lines, n = 43 925, 92 893 and 75 001 for beach, estuary and marina samples, respectively) bacterial operational taxonomic units (OTUs) from beach (blue), estuary (green) and marina (orange) samples. The mean of each distribution was set to equal the average niche optimum, that is the average Eh of the sample where the maximum relative abundance of the OTUs composing the fraction was observed (xmax). The standard deviation was set to equal the average niche breadth defined in this study (dσ) for each community fraction. The height (on the *y*-axis) of each distribution was set to equal the average maximum relative abundance of the OTUs composing the fraction (ymax).

Table 3 The ratio and the mean niche optima (xmax) and breadths (dσ) for the aerophilic and the anaerophilic community fractions of each site

	Beach	Estuary	Marina
Anaerophilic/ Aerophilic ratio	1.70	5.25	2.97
Mean anaerophilic xmax (mV)	−132.5 ± 0.2	−158.2 ± 0.2	−154.6 ± 0.2
Mean anaerophilic dσ (mV)	71.8 ± 0.22	62.28 ± 0.18	65.7 ± 0.21
Mean aerophilic xmax (mV)	220 ± 0.7	130.4 ± 0.9	122.3 ± 0.8
Mean aerophilic dσ (mV)	108 ± 0.3	136.3 ± 0.4	125.5 ± 0.4

Standard deviation is given after the ± symbol.

less over time (quadratic community similarity decay, a = 0.011, b = −0.825, c = 35.09, R^2 = 0.227, n = 184, P = 4.85E−12 for estuary and a = 0.033, b = −1.711, c = 38.986, adjusted R^2 = 0.646, n = 175, P = 2.2E−16 for marina samples, respectively; Fig. 4A, middle and right for estuary and marina samples, respectively), had higher community resistance scores than the beach (0.586 and 0.388 respectively), and the ROM/LOM ratio in the organically enriched samples differed significantly from the expected ratio if no LOM degradation occurred (Wilcoxon tests, normal appr. z = 4.32 and 4.27, $P \ll 0.001$ for estuary and marina, respectively; Fig. 4B, middle and right for estuary and marina samples, respectively), suggesting an effective catabolism of the added organic matter.

An alternative way to measure community resistance

We initially measured community resistance using the equation presented by Shade *et al.* (2012):

$$RS = 1 - 2 \mid y_0 - y_L \mid /(y_0 + \mid y_0 - y_L \mid), \qquad (1)$$

where y_n is a relevant community parameter measured at a time t_n (Shade *et al.* 2012). In our case, the measured parameter is the Bray–Curtis similarity, measured at the beginning and at the end of the incubation. Notably, eqn 1 only takes into account the initial and final averages of community similarity. Meanwhile our results suggest that community similarity may not always decrease at the same rate among different communities (generalized linear model, Supporting Information and Fig. 4A). That has implications regarding the sensitivity of a community to environmental selection; for example, even if the decrease in similarity during a given time period after a disturbance is the same for communities following either exponential or quadratic decay trends, the former trend is indicative of a community that changed faster. Therefore, we propose that the rate of the decay should be included in calculating community resistance: calculate the integral of the equation that best fits the similarity decay and divide it by the product of the initial fitted community similarity and time

$$R = \frac{\int_0^{t_f} f(t)\mathrm{d}t}{f(0) \times t_f} \qquad (2)$$

where R is the community resistance, t is the time, t_f is the duration of the experiment and $f(t)$ is a function explaining a significant part of the variation of community similarity, or any other community metric, over time. If we apply our data to eqn 2, we calculate the community resistance of beach, marina and estuary samples as 0.507, 0.587 and 0.735, respectively. Overall, these results are qualitatively similar to those obtained using eqn 1; however, the community resistance value for marina samples is closer to that of the beach than of

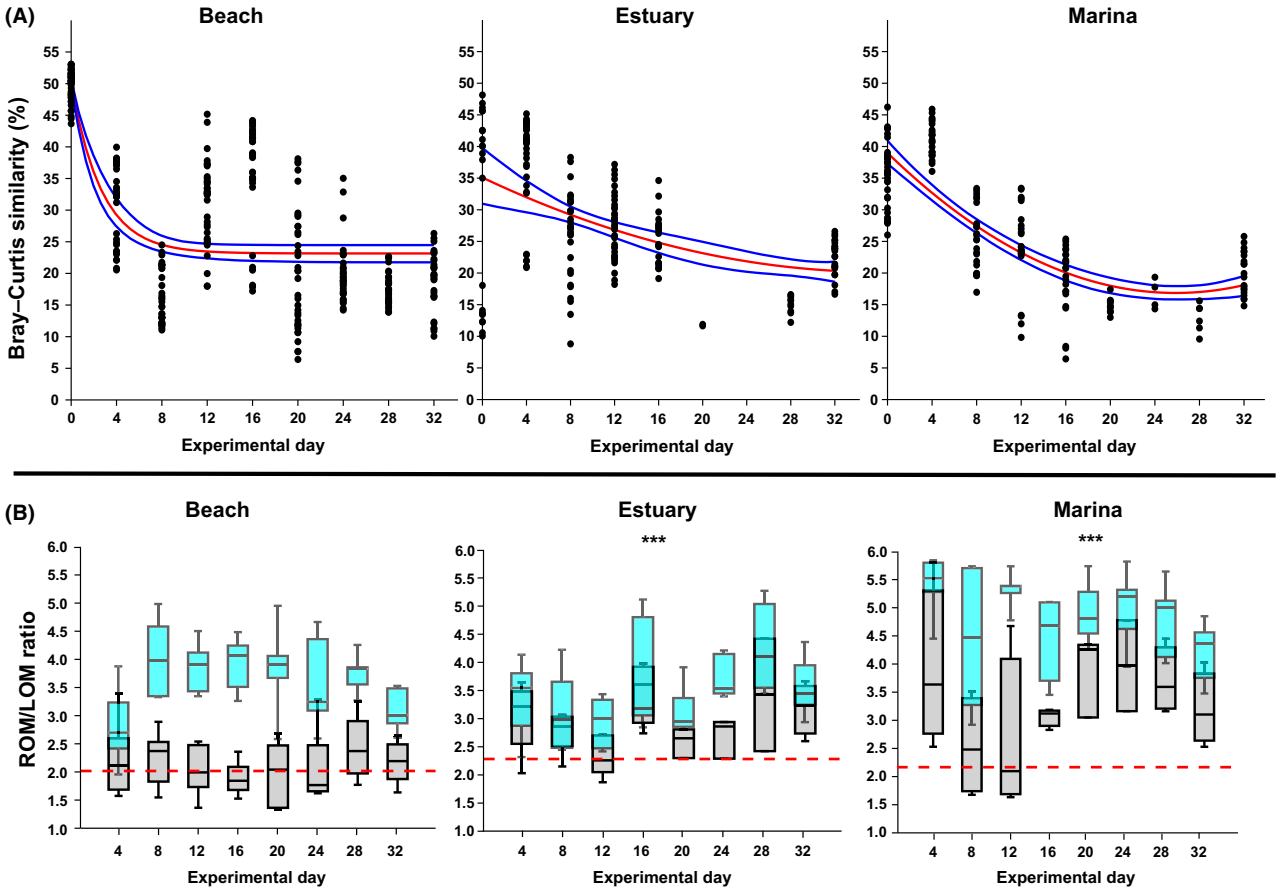

Fig. 4 The structural and functional responses of bacterial communities to organic matter loading. (A) Community similarity decay during the experiment. Model curves are in red, while blue lines represent the 95% confidence intervals of the models. (B) Ecosystem functioning as assessed by the LOM/ROM ratio. Grey boxes (25th–75th percentiles) stand for organically enriched samples, and turquoise boxes stand for nonenriched samples. The dashed red line represents the expected ROM/LOM ratio if no degradation of LOM occurred (R_e). The '***' sign indicates a significant difference (Wilcoxon test, $P < 0.001$) between the ROM/LOM ratio of organically enriched samples and R_e.

the estuary, due to the rapid similarity decay for the marina during the first 20 experimental days (Fig. 4A, right side).

Discussion

Modified niche optima and breadths can explain the historical contingency of bacterial structural and functional community responses

Our results indicate that the communities at the estuary and marina are expected to change less and catabolize organic matter more efficiently, compared with the communities at the beach, in the case of future fluctuations in organic matter and/or oxygen availability within the sediment. This confirms our first hypothesis that environmental history can constrain the structural and functional responses to eutrophication in coastal sediments, because the estuary and the marina are historically more fluctuating and loaded than the beach in terms of chl-α in the water column. Our results widen the existing knowledge of historical environmental constraints on bacterial community responses in other habitats and disturbances (Bouskill *et al.* 2013; Peralta *et al.* 2013, 2014a), for coastal sediments and eutrophication. Nevertheless, future studies that include more sites could further verify our results, as our study included two high-disturbance sites (the estuary and the marina) but only one low-disturbance site (the beach).

Except from historical environmental constraints on community responses, we also found that communities from the beach contained aerophilic bacteria with little tolerance for decreased Eh and with a strong preference for oxic environments, while that was not the case for the marina and estuary communities. This indicates that the aerophilic bacteria in the estuary and the marina communities can better cope with the decreasing Eh in the sediment during a future eutrophication event,

compared with the respective bacteria in the beach community. Interestingly, the magnitude of organic matter addition in our experiment resembles sedimentation rates beneath fish farms or mussel rafts (Valdemarsen *et al.* 2010), which are usually very eutrophic throughout the year, representing a scenario of intense future anthropogenic disturbance. Thus, the estuary and marina communities are expected to be more functional and more stable than the beach community during future eutrophication events, until the sediment becomes highly hypoxic and the anaerophilic bacteria dominate the communities. This confirms our second hypothesis and implies the modification of the niche optima and breadths of the bacterial taxa as a possible mechanism behind the historical environmental contingency of the community responses to eutrophication.

Such mechanistic evidence that links the variability in community responses to environmental preferences of the community members is limited in the literature. Lennon *et al.* have mapped the environmental preferences of 23 bacterial and 22 fungal strains by cultivating them as pure cultures along a moisture gradient in artificial soil (Lennon *et al.* 2012). This method cannot be applied in complex communities *de facto* because of the enormous taxonomic diversity of bacteria within most environmental samples and the lack of cultivability of most community members. More recently, Hawkes and Keitt showed *in silico* that communities forming through arrival of taxa with random niche parameters and different environmental fluctuations had historically constrained functionalities (i.e. substrate utilization; Hawkes & Keitt 2015). Our results hint to the same conclusion for real communities, showing that historically constrained communities contain taxa with modified niche breadths and optima as per their environmental history.

Modelling the niche optima and breadths of bacterial taxa along environmental gradients

Using the parameter xmax of our model, the taxa within a community can be categorized into ecologically meaningful fractions, for example alkalinophilic, neutrophilic and acidophilic (Gubry-Rangin *et al.* 2011), if the distribution along a pH gradient is being examined. Then, the community-wise or fraction-wise niche parameters can be calculated and compared among the different sample categories or fractions.

Our model assumes that there is a meaningful link between the environmental gradient and the community. Therefore, additional tests should be applied to ensure the ecological importance of the environmental parameters on which the gradient is based on and of the calculated niche parameters. The importance of the environmental gradient could be examined by testing how much of the community variation is explained by the gradient, using, for example, distance-based redundancy or canonical correspondence analysis (Borcard *et al.* 2011). For the evaluation of the model results, a significant result in a phylogenetic signal test would indicate that the niche parameters are ecologically important because they are phylogenetically conserved; that is, phylogenetically close taxa have more similar niche parameters than expected by chance (Blomberg *et al.* 2003). In our case, the phylogenetic conservatism of the niche optima and breadths regarding Eh is not surprising; redox potential preferences are deeply conserved phylogenetically in microorganisms (Martiny *et al.* 2015). On the other hand, the nonconserved ymax suggests that bacterial niche specialization for oxygen availability does not necessarily correlate with high abundance at the environmental optimum, a fact opposite to the assumption made by many ecological models for resource utilization (Hawkes & Keitt 2015). However, this should be expected in our case, because there is no direct link between oxygen availability and abundance.

Like all the microbial community analyses that are based on 16S rRNA gene amplicon sequencing, the model uses the read counts of each OTU divided by the total sample reads as a proxy for each OTU's relative abundance, and that number can be potentially biased (Schirmer *et al.* 2015). However, the model examines the change in each OTU's relative abundance along the environmental gradient rather than the relative abundance *per se*. This is considered as a measure of beta diversity, and beta diversity measurements are known to be largely unaffected by biases related to 16S rRNA amplicon sequencing (Mariadassou *et al.* 2015). Nevertheless, the relative abundance can only indicate whether a taxon is dominant within a certain community, giving limited information about the ability of a taxon to proliferate in a specific environment. We cannot exclude the possibility that taxa with broad niches dominate a community, but perform poorly in the environment, for example having high relative abundance within a low bacterial density sample. Thus, our modelling approach would benefit from the incorporation of total bacterial abundance so that the niche parameters are based on the absolute, rather than the relative, abundance. A promising emerging technique for high-throughput cell enumeration in soils and sediments is counting by flow cytometry after detachment from the soil/sediment matrix and staining (Frossard *et al.* 2016). The relative abundance profiles obtained from high-throughput 16S amplicon sequencing can be transformed into the absolute abundance first by correcting with the (predicted) number of 16S copies for each OTU [e.g. using the normalize_by_copy_number.py

script of the PICRUSt package (Langille *et al.* 2013)] and then by multiplying with the total bacterial density estimates from flow cytometry. Then, our modelling approach can be applied to calculate the niche parameters of every OTU along environmental gradients.

Implications for future studies

If historical environmental contingencies in bacterial communities are driven by the modification of niche optima and breadths of the bacterial taxa as our results suggest, microbiome engineering (Mueller & Sachs 2015) and artificial selection (Blouin *et al.* 2015) approaches could be used to modify the community-wise bacterial responses. For example, the introduction of pure cultures or mixed consortia of acclimated bacteria from historically fluctuating habitats could improve the community-wise responses of historically stable habitats, provided that the added microorganisms can proliferate in the new habitat. Moreover, experiments similar to ours could identify the responses of bacterial communities to other types of environmental disturbances such as temperature increases, salinity pulses or exposure to contaminants. That could be valuable considering, for example, the global warming effects on cold ecosystems that were not previously exposed to temperature increase (O'Gorman *et al.* 2014), their bacterial communities possibly being nonacclimated. The niche parameters of the bacterial taxa could be modelled in a similar manner and community resistance could be calculated by taking into account the rates of the structural and functional changes and not just the initial and final states of the community.

Finally, predicting future structural and functional community responses based on the environmental history and on the niche parameters of the individual taxa may be more complicated in the cases of severe environmental disturbances. These types of disturbances often cause regime shifts and lead to alternative stable states (Scheffer *et al.* 2001), such as at the increasingly frequent eutrophication and hypoxia events at the Chesapeake Bay (Kemp *et al.* 2005) and Kattegat (Karlson *et al.* 2002). In these cases where the community is dominated by anaerophiles that push the system further towards hypoxia/anoxia with various feedback mechanisms (Diaz & Rosenberg 2008), disproportionally large environmental changes may be required for the community to return back to its predisturbance state.

Acknowledgements

S.F., G.M. and D.D. were supported by funding from King Abdullah University of Science and Technology (KAUST). The sequencing conducted by the U.S. Department of Energy Joint Genome Institute was supported by the Office of Science of the U.S. Department of Energy under Contract No. DE-AC02-05CH11231. The authors would like to thank Dr. Konstantinos Mavrommatis, Dr. Tijana Glavina del Rio, Dr. Stephanie Malfatti, Petroutsos Spyros-Jason, Arnaud Pirault and Christina Pavloudi for their valuable assistance during sampling, throughout the experiment and regarding the data analysis. We also thank Dr. Jay Lennon, Dr. Marco Fusi and Dr. Pavel Kratina for comments on an earlier version of the manuscript.

Conflict of interest

The authors declare no conflict of interest.

References

Barbier EB, Hacker SD, Kennedy C, Koch EW, Stier AC, Silliman BR (2010) The value of estuarine and coastal ecosystem services. *Ecological Monographs*, **81**, 169–193.

Blomberg SP, Garland T Jr, Ives AR (2003) Testing for phylogenetic signal in comparative data: behavioral traits are more labile. *Evolution*, **57**, 717–745.

Blouin M, Karimi B, Mathieu J, Lerch TZ (2015) Levels and limits in artificial selection of communities. *Ecology Letters*, **18**, 1040–1048.

Borcard D, Gillet F, Legendre P (2011) *Numerical Ecology with R*. Springer, Berlin.

Bouskill NJ, Lim HC, Borglin S *et al.* (2013) Pre-exposure to drought increases the resistance of tropical forest soil bacterial communities to extended drought. *ISME Journal*, **7**, 384–394.

Büchi L, Vuilleumier S (2014) Coexistence of specialist and generalist species is shaped by dispersal and environmental factors. *American Naturalist*, **183**, 612–624.

Caporaso JG, Kuczynski J, Stombaugh J *et al.* (2010) QIIME allows analysis of high-throughput community sequencing data. *Nature Methods*, **7**, 335–336.

Caporaso JG, Lauber CL, Walters WA *et al.* (2011) Global patterns of 16S rRNA diversity at a depth of millions of sequences per sample. *Proceedings of the National Academy of Sciences*, **108**, 4516–4522.

Caporaso JG, Paszkiewicz K, Field D, Knight R, Gilbert JA (2012) The Western English Channel contains a persistent microbial seed bank. *ISME Journal*, **6**, 1089–1093.

Clarke K, Warwick R (2001) *Change in Marine Communities: An Approach to Statistical Analysis and Interpretation*. PRIMER-E, Plymouth, UK.

Diaz RJ, Rosenberg R (2008) Spreading dead zones and consequences for marine ecosystems. *Science*, **321**, 926–929.

Doblin MA, van Sebille E (2016) Drift in ocean currents impacts intergenerational microbial exposure to temperature. *Proceedings of the National Academy of Sciences of the United States of America*, **113**, 5700–5705.

Dornsiepen UF, Manutsoglu E (1994) Zur Gliederung der Phyllit-Decke Kretas und des Peloponnes. *Zeitschrift der Deutschen Geologischen Gesellschaft*, **145**, 286–304.

Edgar RC (2010) Search and clustering orders of magnitude faster than BLAST. *Bioinformatics*, **26**, 2460–2461.

Frossard A, Hammes F, Gessner MO (2016) Flow cytometric assessment of bacterial abundance in soils, sediments and sludge. *Frontiers in Microbiology*, **7**, 903, doi: 10.3389/fmicb.2016.00903.

Furukawa Y, Smith AC, Kostka JE, Watkins J, Alexander CR (2004) Quantification of macrobenthic effects on diagenesis using a multicomponent inverse model in salt marsh sediments. *Limnology and Oceanography*, **49**, 2058–2072.

Good IJ (1953) The population frequencies of species and the estimation of population parameters. *Biometrika*, **40**, 237–264.

Gubry-Rangin C, Hai B, Quince C *et al.* (2011) Niche specialization of terrestrial archaeal ammonia oxidizers. *Proceedings of the National Academy of Sciences of the United States of America*, **108**, 21206–21211.

Hammer Ø, Harper DAT, Ryan PD (2001) Past: paleontological statistics software package for education and data analysis. *Palaeontologia Electronica*, **4**, XIX–XX.

Hanson CA, Fuhrman JA, Horner-Devine MC, Martiny JB (2012) Beyond biogeographic patterns: processes shaping the microbial landscape. *Nature Reviews Microbiology*, **10**, 497–506.

Hawkes CV, Keitt TH (2015) Resilience vs. historical contingency in microbial responses to environmental change. *Ecology Letters*, **18**, 612–625.

Hu C, Lee Z, Franz B (2012) Chlorophyll-a algorithms for oligotrophic oceans: a novel approach based on three-band reflectance difference. *Journal of Geophysical Research*, **117**, C01011, doi: 10.1029/2011JC007395.

Karlson K, Rosenberg R, Bonsdorff E (2002) Temporal and spatial large-scale effects of eutrophication and oxygen deficiency on benthic fauna in Scandinavian and Baltic waters: a review. *Oceanography and Marine Biology*, **40**, 427–489.

Kembel SW, Cowan PD, Helmus MR *et al.* (2010) Picante: R tools for integrating phylogenies and ecology. *Bioinformatics*, **26**, 1463–1464.

Kemp WM, Boynton WR, Adolf JE *et al.* (2005) Eutrophication of Chesapeake Bay: historical trends and ecological interactions. *Marine Ecology Progress Series*, **303**, 1–29.

Klindworth A, Pruesse E, Schweer T *et al.* (2013) Evaluation of general 16S ribosomal RNA gene PCR primers for classical and next-generation sequencing-based diversity studies. *Nucleic Acids Research*, **41**, e1, doi: 10.1093/nar/gks808.

Krom MD, Thingstad TF, Brenner S *et al.* (2005) Summary and overview of the CYCLOPS P addition Lagrangian experiment in the Eastern Mediterranean. *Deep Sea Research Part II: Topical Studies in Oceanography*, **52**, 3090–3108.

Langenheder S, Ragnarsson H (2007) The role of environmental and spatial factors for the composition of aquatic bacterial communities. *Ecology*, **88**, 2154–2161.

Langenheder S, Berga M, Östman Ö, Székely AJ (2011) Temporal variation of β-diversity and assembly mechanisms in a bacterial metacommunity. *The ISME journal*, **6**, 1107–1114.

Langille MGI, Zaneveld J, Caporaso JG *et al.* (2013) Predictive functional profiling of microbial communities using 16S rRNA marker gene sequences. *Nature Biotechnology*, **31**, 814–821.

Lennon JT, Aanderud ZT, Lehmkuhl BK, Schoolmaster DR (2012) Mapping the niche space of soil microorganisms using taxonomy and traits. *Ecology*, **93**, 1867–1879.

Lindström ES, Langenheder S (2012) Local and regional factors influencing bacterial community assembly. *Environmental Microbiology Reports*, **4**, 1–9.

Loh PS, Miller AEJ, Reeves AD, Harvey SM, Overnell J (2008) Assessing the biodegradability of terrestrially-derived organic matter in Scottish sea loch sediments. *Hydrology and Earth System Sciences*, **12**, 811–823.

Mariadassou M, Pichon S, Ebert D (2015) Microbial ecosystems are dominated by specialist taxa. *Ecology Letters*, **18**, 974–982.

Martiny JB, Jones SE, Lennon JT, Martiny AC (2015) Microbiomes in light of traits: a phylogenetic perspective. *Science*, **350**, aac9323, doi: 10.1126/science.aac9323.

Mueller UG, Sachs JL (2015) Engineering microbiomes to improve plant and animal health. *Trends in Microbiology*, **23**, 606–617.

Nemergut DR, Schmidt SK, Fukami T *et al.* (2013) Patterns and processes of microbial community assembly. *Microbiology and Molecular Biology Reviews*, **77**, 342–356.

O'Gorman EJ, Benstead JP, Cross WF *et al.* (2014) Climate change and geothermal ecosystems: natural laboratories, sentinel systems, and future refugia. *Global Change Biology*, **20**, 3291–3299.

Oksanen J, Blanchet FG, Kindt R *et al.* (2013) *vegan: Community Ecology Package*.

Peralta AL, Ludmer S, Kent AD (2013) Hydrologic history influences microbial community composition and nitrogen cycling under experimental drying/wetting treatments. *Soil Biology and Biochemistry*, **66**, 29–37.

Peralta AL, Ludmer S, Matthews JW, Kent AD (2014a) Bacterial community response to changes in soil redox potential along a moisture gradient in restored wetlands. *Ecological Engineering*, **73**, 246–253.

Peralta AL, Stuart D, Kent AD, Lennon JT (2014b) A social–ecological framework for "micromanaging" microbial services. *Frontiers in Ecology and the Environment*, **12**, 524–531.

R Development Core Team (2014) *R: A Language and Environment for Statistical Computing*. R Foundation for Statistical Computing, Vienna, Austria.

Roose-Amsaleg CL, Garnier-Sillam E, Harry M (2001) Extraction and purification of microbial DNA from soil and sediment samples. *Applied Soil Ecology*, **18**, 47–60.

Scheffer M, Carpenter S, Foley JA, Folke C, Walker B (2001) Catastrophic shifts in ecosystems. *Nature*, **413**, 591–596.

Schirmer M, Ijaz UZ, D'Amore R, Hall N, Sloan WT, Quince C (2015) Insight into biases and sequencing errors for amplicon sequencing with the Illumina MiSeq platform. *Nucleic Acids Research*, **43**, e37, doi: 10.1093/nar/gku1341.

Shade A, Peter H, Allison SD *et al.* (2012) Fundamentals of microbial community resistance and resilience. *Frontiers in Microbiology*, **3**, 417, doi: 10.3389/fmicb.2012.00417.

Sogin ML, Morrison HG, Huber JA *et al.* (2006) Microbial diversity in the deep sea and the underexplored "rare biosphere". *Proceedings of the National Academy of Sciences of the United States of America*, **103**, 12115–12120.

Srivastava DS, Kratina P (2013) Is dispersal limitation more prevalent in the ocean? *Oikos*, **122**, 298–300.

Valdemarsen T, Kristensen E, Holmer M (2009) Metabolic threshold and sulfide-buffering in diffusion controlled marine sediments impacted by continuous organic enrichment. *Biogeochemistry*, **95**, 335–353.

Valdemarsen T, Kristensen E, Holmer M (2010) Sulfur, carbon, and nitrogen cycling in faunated marine sediments impacted by repeated organic enrichment. *Marine Ecology Progress Series*, **400**, 37–53.

Vellend BM (2010) Conceptual synthesis in community ecology. *The Quarterly Review of Biology*, **85**, 183–206.

Whitman WB, Coleman DC, Wiebe WJ (1998) Prokaryotes: the unseen majority. *Proceedings of the National Academy of Sciences of the United States of America*, **95**, 6578–6583.

Wildish D, Akagi H, Hamilton N, Hargrave B (1999) A recommended method for monitoring sediments to detect organic enrichment from mariculture in the Bay of Fundy. *Canadian Technical Report of Fisheries and Aquatic Sciences*, **2286**.

Wollenhaupt N, Wolkowski R (1994) Grid soil sampling. *Better Crops*, **78**, 6–9.

Zachariasse WJ, van Hinsbergen DJJ, Fortuin AR (2008) Mass wasting and uplift on Crete and Karpathos during the early Pliocene related to initiation of south Aegean left-lateral, strike-slip tectonics. *Geological Society of America Bulletin*, **120**, 976–993.

Zinger L, Boetius A, Ramette A (2014) Bacterial taxa-area and distance-decay relationships in marine environments. *Molecular Ecology*, **23**, 954–964.

ZoBell CE (1946) Studies on redox potential of marine sediments. *AAPG Bulletin*, **30**, 477–513.

E.D.L., I.K. and S.F. designed the experiment; S.F., N.P., O.M. and I.T. performed the experiment and collected the raw data; S.F., A.M. and G.M. performed the analyses; A.M., G.M. and D.D. provided new methods and materials; S.F. wrote the first version of the manuscript; and all authors contributed to revisions.

Data accessibility

Raw sequence data were submitted to the Short Read Archive (SRA) section of the NCBI database under the alias SRA16686.

Supporting information

Additional supporting information may be found in the online version of this article.

Fig. S1 Eh values (Y axis) over time (t1-t8, X axis) for samples originating from the beach.

Fig. S2 Eh values (Y axis) over time (t1-t8, X axis) for samples originating from the marina.

Fig. S3 Eh values (Y axis) over time (t1-t8, X axis) for samples originating from the estuary.

Fig. S4 Sulphide emission (Y axis) over time (t1-t8, X axis) for samples originating from the beach.

Fig. S5 Sulphide emission (Y axis) over time (t1-t8, X axis) for samples originating from the marina.

Fig. S6 Sulphide emission (Y axis) over time (t1-t8, X axis) for samples originating from the estuary.

Fig. S7 25-75% percentile comparison boxplots of dissolved oxygen concentration, in microcosms with (Treatments 1/2 – grey boxes) and without (Treatments 3/4 –white boxes) organic enrichment.

Fig. S8 The sampling map of the sites where sediment was originally collected from, with the island of Crete (bottom) and a focus to the specific area where the three different sites are located (above).

Fig. S9 Schematic representation of the microcosm experimental design.

Table S1 Normality tests for the satellite data values of chlorophyll-α.

Table S2 The distribution of the samples that were included in the analysis based on the site of origin and incubation conditions.

Table S3 Model fit (AIC) regarding the BC community similarity decay through time for the samples from each site.

Table S4 Welch test comparisons of the niche parameters among the different community fractions (aerophilic and anaerophilic OTUs) from the different sites.

Table S5 The results of the general additive model regarding the community similarity decay over time for the communities from each site.

Table S6 Distance-based canonical correspondence analysis (db-cca) results.